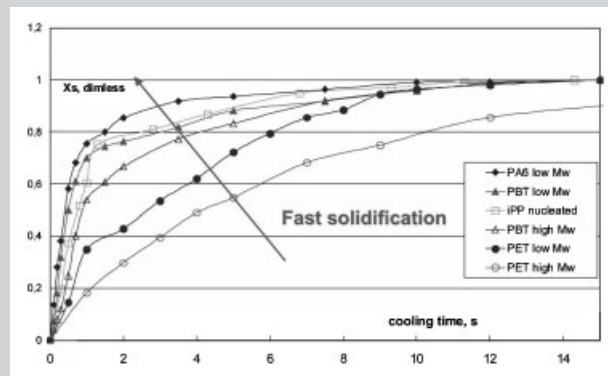


**Summary:** An in-line method for monitoring the solidification process during injection molding of semicrystalline polymers (demonstrated previously in *J. Appl. Polym. Sci.* **2003**, *89*, 3713) is based on a simple device, where an additional ejector pin is pushed on the injection molded part at different times during the solidification phase. The ‘indentation depth profile’, i.e., residual deformation as a function of time, was obtained and allowed to determine the evolution of the solidification front in the mold as a function of the cooling time. The present work shows the reliability and the powerfulness of the aforementioned method for a large variety of different semicrystalline polymers (PET, PBT, polyamide-6 PA6, isotactic poly(propylene) iPP) characterized also by different molecular weight and/or nucleating agents. The results show that the indentation test may be considered as a ‘predictive’ tool to qualitatively and quantitatively compare the solidification process of different polymers and polymer grades during injection molding.



Comparison of the solid front propagation during injection molding of different materials.

# The Use of the Indentation Test for Studying the Solidification Behaviour of Different Semicrystalline Polymers during Injection Molding

Vincenzo La Carrubba,\*<sup>1</sup> Wouter Gabriëlse,<sup>2</sup> Stefano Piccarolo<sup>1</sup>

<sup>1</sup>DICPM, University of Palermo, Viale delle Scienze, 90128, Palermo, Italy  
E-mail: lacarrubba@dicpm.unipa.it

<sup>2</sup>DSM Engineering plastics, P.O. Box 18, 6160 MD, Geleen, The Netherlands

Received: June 15, 2005; Revised: August 4, 2005; Accepted: August 29, 2005; DOI: 10.1002/mame.200500216

**Keywords:** injection molding; processing; semicrystalline polymers; thermoplastics

## Introduction

The injection molding process of thermoplastic polymers mainly consists of four stages: filling (the material is injected into the cavity), packing/holding (additional molten material is forced into the cavity to compensate for shrinkage), cooling (part solidifies) and ejection. Generally speaking, from a technological viewpoint an optimisation of the injection molding process should focus mainly on the reduction of the cooling time, which is the longest part of the total injection molding cycle time; this is particularly true for molded parts in industrial processes, normally characterized by relatively large shot volumes and thick walls. Figure 1 shows a schematic representation of the typical times each stage contributes to in the injection molding of crystallizing polymers. Although the cooling process

starts already when the polymer melt gets in contact with the cold wall, i.e. during the injection stage, the conventional definition of the “cooling stage” is based on the time when gate freeze-off takes place.<sup>[1]</sup> On the other hand, the large number of factors affecting simultaneously final morphology and properties makes very complex the understanding of the global phenomenology occurring during the various stages of the process. With this respect, the possibility to use innovative in-line and on-line techniques to monitor solidification/crystallization phenomena during real processing operations turns out to be the key point for a deeper insight into the investigation of structure development.

Several interesting methods for online monitoring the solidification process have been proposed and implemented so far, either in real processing equipment (such as injection

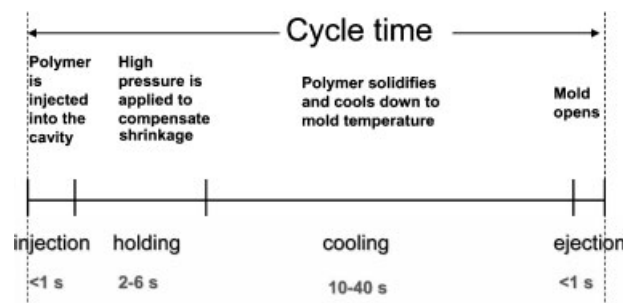


Figure 1. Schematic representation of the injection molding cycle time.

molding machine), or in model experiments aiming to emulate processing conditions. As far as the latter experiments are concerned, it is worth mentioning the use of depolarised light intensity during fast quenching of thin polymeric films, as proposed by Ding and Spruiell<sup>[2]</sup> and, more recently improved by Titomanlio et al.<sup>[3]</sup>

Going to the on-line systems implemented in industrial processes, a method based on an optical sensor measuring reflected light intensity in a transparent injection mold has been proposed by Thomas and Bur.<sup>[4]</sup> Moreover, an ultrasonic monitoring of solidification behaviour of semicrystalline polymers was implemented to describe their Pressure-Volume-Temperature (PVT) behaviour under static conditions, as proposed by Kim et al.<sup>[5]</sup> and under typical injection molding conditions by Smith et al.<sup>[6]</sup> Another potentially promising technique to detect structural changes occurring during crystallization is dielectric spectroscopy, recently implemented in injection molding by Guillet et al.<sup>[7]</sup>

In a previous paper the present authors reported a new in-line technique – the so-called ‘indentation test’ – to monitor the solidification process during the cooling phase of injection molding.<sup>[8]</sup> The method is based on a simple device, where an additional ejector pin is pushed on the injection molded part at different times during the solidification phase, while the mold remains closed and the gate is already frozen in. By performing the indentation at different times during the cooling phase, an indentation depth profile, i.e. residual deformation as a function of time, can be obtained which gives information about the solidification process. The ease of operation, the large applicability to different classes of semicrystalline polymers (polyesters, polyamides, polyolefins) and the simplicity of the interpretation, make the method very useful for a general understanding of the “moldability” of a given material in terms of process cycle time and final properties of the molded part.

The method was demonstrated on a relatively slow crystallizing polymer [poly(ethylene terephthalate), PET], varying in molecular weight, a relatively fast crystallizing polymer [poly(butylene terephthalate), PBT] and a glass

fibre reinforced PET grade (with 30% glass fibres). A simplified two-phase model was proposed to interpret the experimental data where the disappearance of the liquid phase is mainly attributed to transient heat conduction through the thickness of the mold. Based on this model, the propagation rate of the solidification front was derived from the indentation depth profiles and experimental data were compared with predicted data based on a simple heat transfer model.<sup>[8,9]</sup>

Whereas in the previous paper the reliability of the indentation test was demonstrated by applying this method to some “test polymers” (with this respect PET, being slowly crystallizing, was the best candidate to highlight the usefulness of the technique), in this work a more extensive comparative investigation on different materials and material grades is reported (PET, PBT, polyamide-6 PA6, isotactic poly(propylene) iPP), in order to show how the method can be technologically applied to study the solidification behaviour during processing, which, in its turn, is partly responsible for the typical cooling times of injection molding.

We highlight the applicability to a vast class of semicrystalline polymers (polyesters, polyamides, polyolefins), whose solidification behaviour under processing conditions can be effectively accounted for. The method accounts and distinguishes not only polymers crystallizing at very different rates, also fast crystallizing ones, more common in the molding industry, can be discriminated.

## Experimental Part

### Materials

Two PET samples, two PBT samples, two PA6 samples and two iPP samples were used to illustrate the applicability of the method. The main material characteristics are reported in Table 1.

### Test Method

Details concerning the method are reported in the previous paper.<sup>[8]</sup> The method was implemented on a standard

Table 1. Main characteristics of the materials studied in this work.

	$\eta_{rel}$	$\bar{M}_n$
PET low $\bar{M}_w$	1.6 <sup>a)</sup>	19 000
PET high $\bar{M}_w$	2 <sup>a)</sup>	33 600
PBT low $\bar{M}_w$	1.93 <sup>a)</sup>	18 500
PBT low $\bar{M}_w$	2.4 <sup>a)</sup>	32 000
PA6 low $\bar{M}_w$	2.2 <sup>b)</sup>	12 000
PA6 high $\bar{M}_w$	3.2 <sup>b)</sup>	25 000
iPP	–	52 000

a) Relative viscosity measured in 1% *m*-cresol.

b) Relative viscosity measured in formic acid.

Table 2. Typical injection molding conditions for the materials used.

	$t_{inj}$	$P_{hold}$	$t_{hold}$	$P_{ind.}$	$T_m$	$T_w$
	s	bar <sup>b)</sup>	s	bar <sup>a)</sup>	°C	°C
PET low $\bar{M}_w$	0.53	30	3.5	30	285	135
PET high $\bar{M}_w$	0.74	55	5.5	45	285	135
PBT low $\bar{M}_w$	0.6	45	3	34	260	90
PBT high $\bar{M}_w$	0.7	45	2.9	45	260	90
PA6 low $\bar{M}_w$	0.63	38	4	40	260	70
PA6 high $\bar{M}_w$	0.67	45	4	50	260	70
iPP	0.57	20	4	20	250	40
iPP + nucleants	0.42	25	4	20	250	40

a) Pressure values set at the machine. For the equivalent real pressure multiply by 16 (hydraulic plug to front pin surface ratio).

b) Pressure values set at the machine. For the equivalent real pressure multiply by 13.

multipurpose injection molding machine with typical operating conditions (see Table 2). A two-cavity mold was adopted, each cavity being of rectangular shape, as shown in Figure 2, reporting cavity length and width. Cavity thickness was 1.6 mm. In one of the two cavities, 12 mm apart from the cavity edge, opposite to the gate, a pressure sensor was installed, which allowed the pressure trace in the cavity to be recorded during the process (see Figure 2).

After the packing phase has been completed, i.e. after the gate is frozen,<sup>[8]</sup> an “indentation” pin is pushed towards the sample surface with a constant controllable pressure, causing the pin to penetrate within the polymer. Irrespective to the polymer used for the test, by performing the indentation at different times an ‘indentation depth profile’ is obtained as schematically shown in Figure 3a. The initial point of the curve reported in Figure 3a at time zero, represents the maximum indentation depth ( $\delta_{max}$ ) recorded at the end of the packing

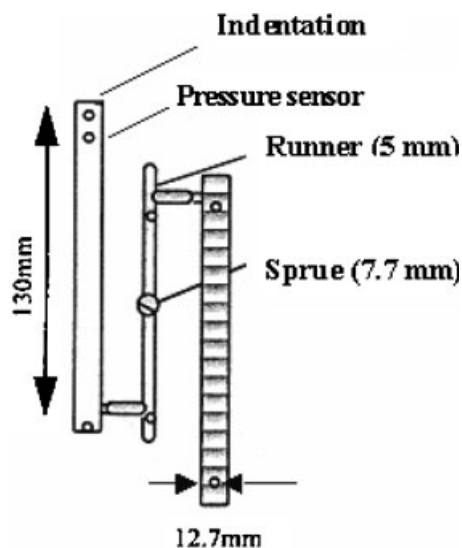


Figure 2. Mold used for the indentation test.

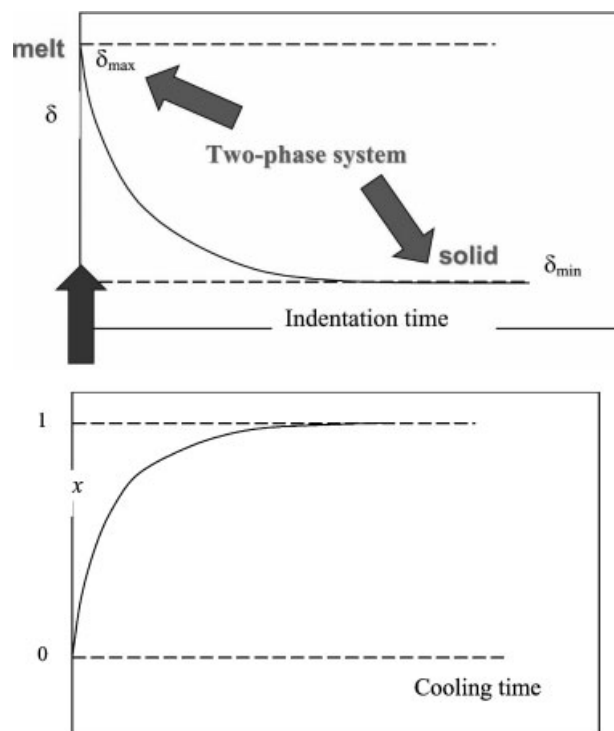


Figure 3. (a, topmost) Indentation depth profile. (b, bottommost) Solid layer evolution as derived from the indentation test profile.

phase, where the polymer is mostly in the molten state. With increasing cooling time, the amount of solid phase increases. This will lead to a gradual decrease in indentation depth, reaching a final value ( $\delta_{min}$ ), where the material has been completely solidified. The indentation depth is related to the compressibility of the material inside the cavity that consists of two phases, a solidified one and a phase, which up to  $\delta_{min}$  is still liquid. The total compressibility depends on the volume weighed compressibility of both phases.

The two basic assumptions<sup>[8]</sup> made for the interpretation of the indentation test, (i.e. the indentation depth profile is a measure of the response of a two-phase system and the stress state induced by the pin indentation is to a large extent a “pure” compression state, being the shear strength of both the solid and molten phases negligible with respect to the bulk strength) lead to the following result for the volumetric solid fraction,  $x_s$ :

$$x_s(t) = \frac{\delta(t) - \delta_{max}}{\delta_{min} - \delta_{max}} \quad (1)$$

Hence, from the curves reporting  $\delta$  versus time (Figure 3a), the evolution of  $x_s$  as a function of time can be derived using Equation (1), which represents a sort of “normalization” procedure to work out the solid fraction on the basis of the maximum and minimum indentation depth, as schematically shown in Figure 3b.

$\delta_{max}$ , the maximum indentation depth, is proportional to the compressibility of the liquid phase whereas  $\delta_{min}$ , the minimum indentation depth, is proportional to the compressibility of the solid phase.<sup>[8,10]</sup>

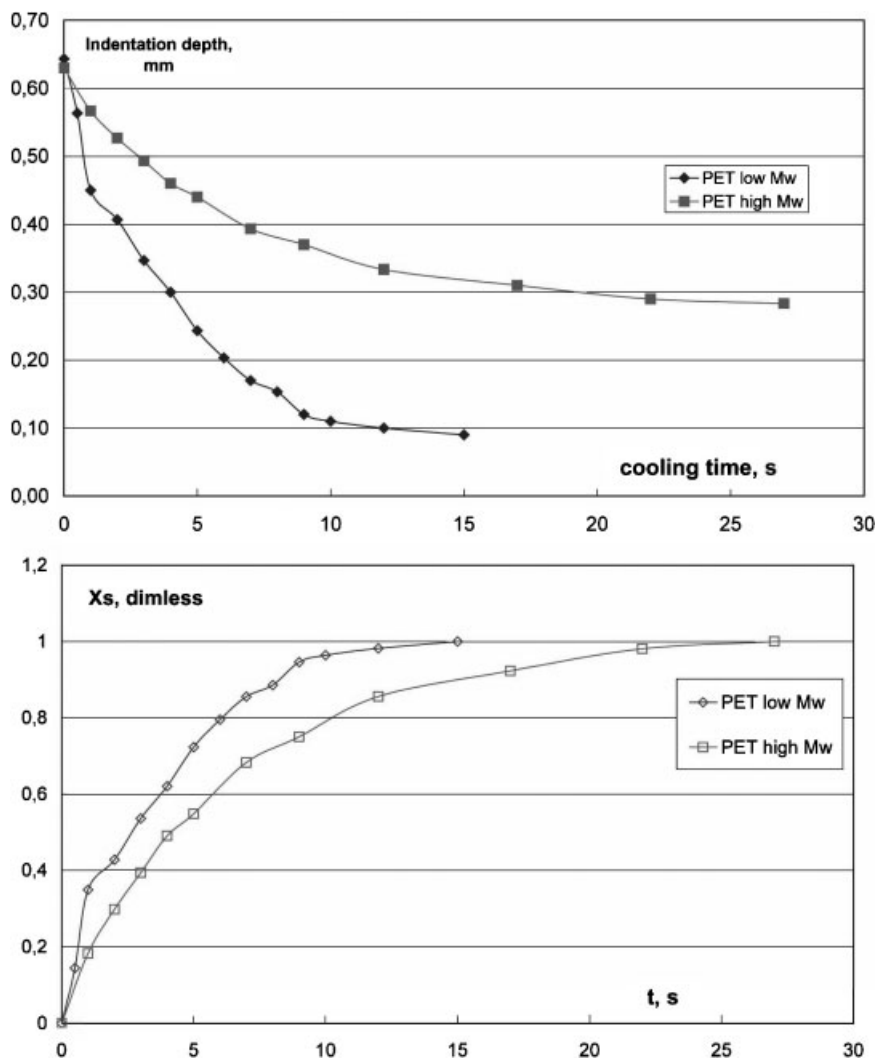


Figure 4. (a, top) Indentation test profiles for two PETs with different  $\bar{M}_w$ ; (b, bottom) Solid front propagation for two PETs with different  $\bar{M}_w$ .

## Results and Discussion

The indentation test profiles  $\delta(t)$  for two PET grades characterized by different molecular weights are reported in Figure 4a. The solid layer evolution as a function of time, as derived from the indentation tests according to Equation (1), is reported in Figure 4b.

It should be noticed that the “normalized” indentation depth profile leading to the volumetric solid fraction as a function of time (Equation (1)), is based on the assumption that the indentation depth (hence material compressibility) undergoes an abrupt change at a given temperature  $T_c$ , which determines a transition from melt to solid. Hence the crystallization kinetics is not considered. As it can be noticed from Figure 4a and b, these two materials reveal a different solidification behaviour. In particular, the high molecular weight PET exhibits a slower decay of indentation depth to be related with the slower solidification

behaviour than the low molecular weight grade, in agreement with known dependence on molecular weight of overall crystallization kinetics.<sup>[11]</sup> This result shows that the indentation test is able to discriminate between the two PET grades characterized by different molecular weights, since they exhibit different solidification behaviour.

It should be however underlined that the method is not suitable to determine the crystallization kinetics, but it is able to quantitatively discriminate between different material features, the differences being technologically relevant for product development.

The solid layer evolution as a function of time, as derived from the indentation tests according to Equation (1) for two PBT grades characterized by different molecular weights is reported in Figure 5, whereas Figure 6 shows the solid layer evolution for two PA6 grades, a low and a high molecular weight. In both cases it appears that the general trend of the curves is quite different for the two material grades, being

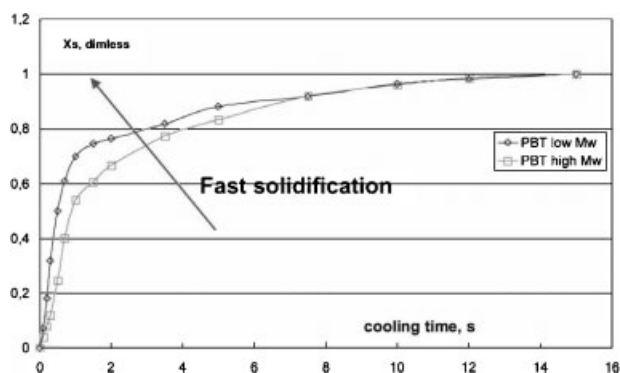


Figure 5. Solid front propagation for two PBTs with different  $\bar{M}_w$ .

the two curves clearly distinct from each other. As a matter of fact the high molecular weight PBT and PA6 exhibit a slower solidification behaviour than the low molecular weight grades. This result confirms that the indentation test is able to discriminate between the two PBT/PA6 grades characterized by different molecular weights, since they exhibit different solidification behaviour.

Furthermore, a comparison of Figure 4 with Figure 5 and 6 shows that the differences between the two PET materials are more remarkable than the ones noticeable for the two PBTs and the two PA6s, highlighting that the influence of molecular weight on the crystallization behaviour of a slowly crystallizing polymer is greater than of a fast crystallizing one (PET vs. PBT and PA6), as already outlined by many published works.<sup>[11–14]</sup>

Finally, an analysis of Figure 5 and 6 demonstrates that the difference between the two PA6s is about of the same order of magnitude as the difference of the two PBTs, further supporting the evidence that the crystallization rates of PA6 and PBT under typical processing conditions are comparable and some orders of magnitude larger than PET.<sup>[12,15–17]</sup>

The effect of nucleating agents on the solidification behaviour of iPP can be easily observed by looking at Figure 7 reporting the “normalized” solidification profiles derived

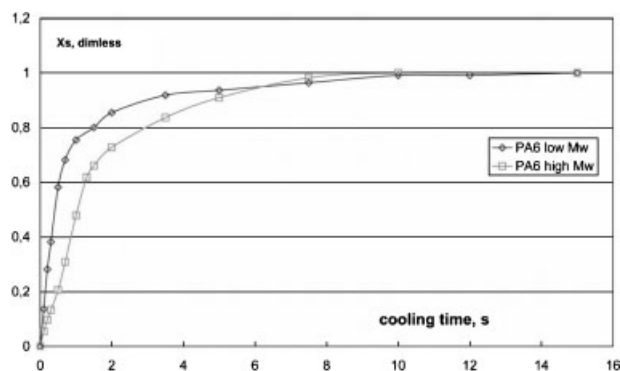


Figure 6. Solid front propagation for two PA6s with different  $\bar{M}_w$ .

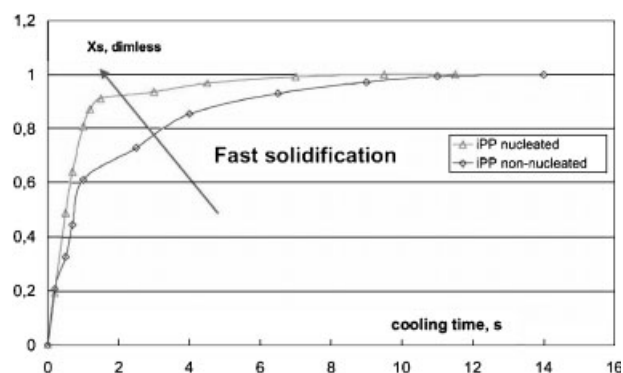


Figure 7. Solid front propagation for two iPPs with and without nucleants.

from indentation tests performed on a nucleated and non-nucleated iPP. Nucleating agents clearly determine an acceleration of iPP crystallization, as already reported by several authors.<sup>[18,19]</sup>

A comparison of the solid layer evolution as a function of time, as derived from the indentation tests performed on all the aforementioned materials is reported in Figure 8. This picture shows that the indentation test allows one to explore the crystallization behaviour during processing of a wide range of materials (polyesters, polyamides, polyolefins), even accounting for changes on molecular weight and presence of nucleating agents. The observed behaviour confirms that solidification in real injection molding conditions is a very fast process for PA6, iPP and low  $\bar{M}_w$  PBT, it becomes slower for a high  $\bar{M}_w$  PBT, and finally it becomes very slow for PET (for this material the higher the molecular weight, the slower the process).

Figure 9 shows also that the heat penetration theory, which predicts a square root dependence of the solid front on cooling time, applies for all the materials investigated in this work.

As a matter of fact according to the theory of heat penetration,<sup>[9]</sup> assuming that solidification occurs at a given temperature  $T_c$ , the relationship between the position where the solidification front is located and the time at which the

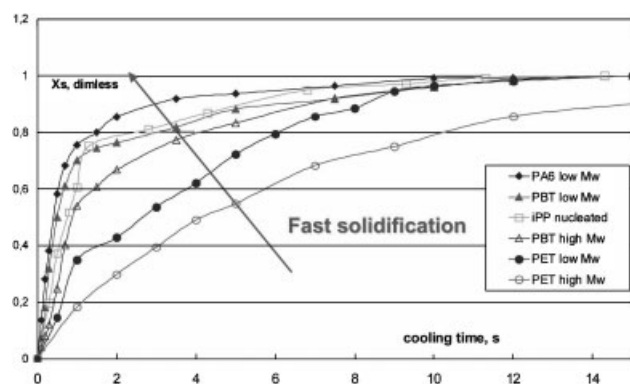


Figure 8. Comparison of the solid front propagation for different materials.



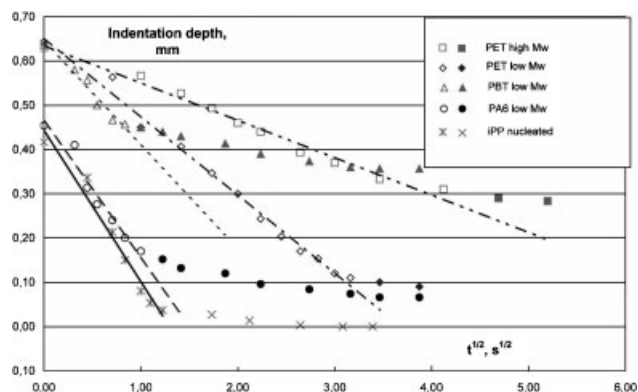


Figure 9. Indentation depth as a function of square root of time (various materials).

solidification occurred, is governed by the equation:

$$x = (K \times 2 \times \sqrt{\alpha}) \times \sqrt{t} \quad (2)$$

with  $\alpha$  = polymer thermal diffusivity and  $K$  = a constant depending on melt temperature, mold temperature and crystallization temperature.<sup>[8]</sup> By rewriting Equation (1) and substituting  $x_s = \frac{x}{l}$  in Equation (2) ( $l$  = sample half thickness), we also have:

$$\delta(t) = \delta_{\max} + (\delta_{\min} - \delta_{\max})x_s(t) \quad (3)$$

$$\delta(t) = \delta_{\max} + (\delta_{\min} - \delta_{\max}) \left[ \frac{K2\sqrt{\alpha}}{l} \right] \sqrt{t} \quad (4)$$

that predicts a square root dependence of the indentation depth as a function of time. If one plots  $\delta(t)$  as a function of square root of time, one can determine the intercept giving the initial indentation value ( $\delta_{\max}$ ) and the slope indicating the rate of the solidification front propagation. A complete discussion about the information that can be drawn from Equation (3) and (4) has been extensively reported in the previous paper.<sup>[8]</sup>

From Figure 8 it is also evident that, the slower the crystallization process (e.g. PET), the longer will be the consistency of the square root time dependence, the faster the crystallization (e.g. PA6) the shorter will be the time in which the heat penetration theory is fulfilled.

By using the slope of the curves reported in Figure 9 it is possible to calculate back the value of the constant  $K$  (Equation (4)) for all the materials whose indentation depth profiles were experimentally recorded. The value of the average crystallization temperature of the polymers, lying in the range of typical crystallization temperatures at high cooling rates,<sup>[8,12,15,16,20]</sup> can be obtained. Since mold and melt temperatures are set operating conditions, the determination of the constant  $K$  results into an implicit knowledge of crystallization temperature  $T_c$ .

The crystallization temperatures calculated through this procedure were then compared to temperatures of the

Table 3. Material parameters and crystallization conditions.

	$\alpha^a)$	$T_m$	$T_w$	$T_c^b)$	$T_c^c)$
	$W \cdot mK^{-1}$	$^{\circ}C$	$^{\circ}C$	$^{\circ}C$	$^{\circ}C$
PET low $\bar{M}_w$	$1.6 \times 10^{-7}$	285	135	185	179.3
PET high $\bar{M}_w$	$1.6 \times 10^{-7}$	285	135	175	172.3
PBT low $\bar{M}_w$	$3.8 \times 10^{-7}$	260	90	155	141
PBT high $\bar{M}_w$	$3.8 \times 10^{-7}$	260	90	145	129
PA6 low $\bar{M}_w$	$4 \times 10^{-7}$	260	85	140	134.3
PA6 high $\bar{M}_w$	$4 \times 10^{-7}$	260	85	130	123

a) From literature.

b) Calculated.

c) From DSC.

minima of DSC fast cooling ramps (at  $150^{\circ}C \cdot \text{min}^{-1}$ ). DSC crystallization temperatures during the cooling ramps are reported in Table 3 and compared to crystallization temperatures as calculated from our simplified thermal model applied to indentation test profiles. The maximum possible DSC cooling rate ramp was used to obtain the data of Table 3 in order to make a reasonable comparison with the typical cooling rate range in which crystallization occurs in the bulk of an injection molded sample, i.e. ca few  $^{\circ}C \cdot \text{s}^{-1}$ .<sup>[11]</sup> The comparison reported in Table 3 shows that a reasonable guess of  $T_c$  can already be made on the basis of experimental depth profiles recorded online during the molding cycle.

Finally, it is worth reminding that it has been assumed that solidification or crystallization occurs abruptly at a given temperature  $T_c$  with no other requirement from knowledge of crystallization kinetics but use of the experimental evidence that at high cooling rates crystallization takes place in a narrow range of temperatures, characteristic of a given polymer,<sup>[12,15,16,20]</sup> as it was clearly explained in a previous paper.<sup>[8]</sup> As a matter of fact, this statement finds further support considering that a small crystalline fraction is sufficient to give rise to the onset of solid like behaviour, i.e. gelation.<sup>[1,21]</sup> This observation could justify the slight overestimation of the  $T_c$  supplied by the indentation test with respect to the DSC minima (referring to about 50% of the overall crystalline content).

Although only the first part of the test can rigorously be interpreted on the basis of heat propagation arguments, nevertheless the simplified “compressibility based” modelling represented by Equation (1) makes the method suitable for a comparison on an empirical basis of materials exhibiting similar features in the whole range of cooling times explored.

The present method can thus be used to discriminate between different materials solidification behaviour under conditions experienced in injection molding where a complex set of independent variables determines materials solidification behaviour, often difficult to assess independently by other techniques.

## Conclusion

An on-line technique on injection molding recently proposed,<sup>[8]</sup> the “indentation test”, was extensively performed on different classes of materials (polyesters PET and PBT, polyamides PA6 and polyolefins iPP) characterized by variation in structural parameters (molecular weight and presence of nucleants).

From the shape of the indentation curve obtained, the evolution of the solidification front as a function of time can be determined and a good agreement between experimental data and predictions of the evolution of the solid layer thickness based on the classical theory of heat penetration (without taking into account crystallization kinetics) was obtained. The method appears to be very sensitive to materials adopted, allowing one to discriminate between different polymers (from slowly crystallizing, e.g. PET, to fast crystallizing ones, e.g. PBT, PA6, iPP) and material features (Molecular weight, nucleants). It also allows to indirectly determine the temperature range in which crystallization occurs under typical injection molding conditions, thus confirming previous authors' results. It bridges common molders' practice with knowledge of solidification behaviour under processing conditions, few examples behind any words. The experimental evidence that the solidification rate (and hence cycle time) of PBT and PA6 are comparable, as already shown, and the observation that the larger the crystallization rate (PBT vs. PET) the less relevant the influence of molecular weight are a few successful proofs reported here.

The method can thus be regarded as a reliable and powerful tool to monitor on-line the solidification process during injection molding and may represent an effective method to describe the solidification behaviour under “realistic” operating conditions.

- [1] G. Titomanlio, S. Piccarolo, G. Levati, *J. Appl. Polym. Sci.* **1988**, *35*, 1483.
- [2] Z. Ding, J. Spruiell, *J. Polym. Sci., Part B: Polym. Phys.* **1996**, *34*, 2783.
- [3] G. Lamberti, F. De Santis, A. Giannattanasio, V. Brucato, G. Titomanlio, “*Proc. of PPS 18*”, Guimaraes 2002.
- [4] C. L. Thomas, A. J. Bur, *Polym. Eng. Sci.* **1999**, *39*, 1291.
- [5] J. G. Kim, J. W. Lee, “*Proc. of PPS 18*”, Guimaraes 2002.
- [6] G. D. Smith, E. C. Brown, P. D. Coates, “*Proc. of PPS 18*”, Guimaraes 2002.
- [7] J. Guillet, J. M. Gonnet, I. Sirakov, R. Fulchiron, G. Seytre, “*Proc. of PPS 17*”, Montreal 2001.
- [8] V. La Carrubba, W. Gabriëlse, M. van Gorp, S. Piccarolo, V. Brucato, *J. Appl. Polym. Sci.* **2003**, *89*, 3713.
- [9] R. B. Bird, W. E. Stewart, E. N. Lightfoot, “*Transport Phenomena*”, Wiley, New York 1960.
- [10] “*Kenndaten für die Verarbeitung thermoplastischer Kunststoffe, 1: Thermodynamik*”, Carl Hanser Verlag, München, Wien 1979.
- [11] B. Gumther, H. G. Zachmann, *Polymer* **1983**, *24*, 1008.
- [12] S. Piccarolo, V. Brucato, Z. Kiflie, *Polym. Eng. Sci.* **2000**, *40*, 1263.
- [13] C. Vanderdonckt, M. Krumova, F. J. Baltà Calleja, H. G. Zachmann, S. Fakirov, *Colloids Polym. Sci.* **1998**, *276*, 138.
- [14] Y. Y. Cheng, M. Brillhart, P. Cebe, M. Capel, *J. Polym. Sci., Part B: Polym. Phys.* **1996**, *34*, 2953.
- [15] V. Brucato, G. Crippa, S. Piccarolo, G. Titomanlio, *Polym. Eng. Sci.* **1991**, *31*, 1411.
- [16] V. Brucato, S. Piccarolo, G. Titomanlio, *Int. J. Form. Processes* **1998**, *1*, 35.
- [17] G. Coppolino, personal communication, 1997.
- [18] M. A. Lopez-Manchado, M. Arroyo, *Polymer* **2000**, *41*, 7761.
- [19] K. Nagarajan, K. Levon, A. S. Myerson, *J. Therm. Anal. Calorim.* **2000**, *59*, 497.
- [20] V. Brucato, S. Piccarolo, V. La Carrubba, *Chem. Eng. Sci.* **2002**, *57*, 4129.
- [21] N. V. Pogodina, H. H. Winter, *Macromolecules* **1998**, *31*, 8164.